ELSEVIER

Cardiovascular Research 31 (1996) 953–962

Cardiovascular Research

The vulnerable period for low and high energy T-wave shocks: Role of dispersion of repolarisation and effect of *d*-sotalol

Paulus F. Kirchhof [a,b], C. Larissa Fabritz [a,b], Markus Zabel [a], Michael R. Franz [a,*]

[a] *Cardiology Divisions, Veterans Administrations and Georgetown University Medical Centers, Washington, DC, USA*
[b] *Westfälische Wilhelms-Universität Münster, Münster, Germany*

Received 3 May 1995; accepted 5 February 1996

Abstract

Introduction: The induction of ventricular fibrillation (VF) by T-wave shocks has been related to dispersion of repolarisation, but only indirect evidence of this hypothesis exists. The effects of drugs prolonging repolarisation like *d*-sotalol on the vulnerability to T-wave shocks remain unknown. **Methods:** In 9 isolated rabbit hearts, 7 monophasic action potentials (MAPs) and an ECG were recorded simultaneously. Vulnerable periods were determined using two different shock strengths, one close to the fibrillation threshold and the other close to the upper limit of vulnerability, at baseline and after action potential prolongation by *d*-sotalol. **Results:** The vulnerable period had a duration of 30 ± 14 ms for the lower and 34 ± 12 ms for the higher shock strength (P = NS). Coupling intervals of the vulnerable periods were 13 ± 10 ms shorter for higher shock strengths as compared to lower shock strengths ($P < 0.005$). The vulnerable period for low shock strengths coincided with dispersion of MAPs at 90% repolarisation ($r = 0.87$–0.92, $P < 0.005$), and the vulnerable period for high shock strengths coincided with dispersion at 70% repolarisation ($r = 0.82$–0.93, $P < 0.005$). ECG parameters predicted the vulnerable periods less precisely than MAP repolarisation ($r \leq 0.72$). *d*-Sotalol prolonged MAP durations by an average of 33 ms at 70% and 39 ms at 90% repolarisation but did not alter the described relations, nor did it reduce dispersion of repolarisation or duration of the vulnerable periods. **Conclusions:** Dispersion of repolarisation determines vulnerable periods and might be part of the arrhythmogenic substrate promoting induction of VF by T-wave shocks. The coupling intervals of the vulnerable periods depend on the applied shock strength as well as repolarisation, with shock strengths close to the fibrillation threshold inducing VF during dispersion at 90% repolarisation and shock strengths close to the upper limit of vulnerability inducing VF during dispersion at 70% repolarisation. *d*-Sotalol reduces neither vulnerability to T-wave shocks nor dispersion of repolarisation in this isolated heart model.

Keywords: T-wave shock; Ventricular fibrillation; Repolarisation; Monophasic action potential; Arrhythmias

1. Introduction

The vulnerable period of the heart is known as the time interval during which electrical stimuli induce ventricular fibrillation (VF) [1]. The development of the automatic cardioverter defibrillator and the correlation of the upper limit of vulnerability (ULV) with the defibrillation threshold have renewed interest in the vulnerability of the heart to high energy shocks and have led to studies of the vulnerable period for single T-wave shocks [2–4]. The vulnerable period for T-wave shocks has been found to coincide with the ascending [4], and to some extent the descending [5], limb of the T-wave of the surface ECG. This finding concurs with the hypothesis that the vulnerability of the heart relates to the late repolarisation phase of the action potential [6,7]. However, this hypothesis has not yet been directly tested.

Previous studies referred to a single vulnerable period, usually determined for an arbitrary stimulus strength [2,6]. According to the strength–interval relation [8,9], a stronger stimulus excites the heart at earlier repolarisation states. If translated to field shock stimuli, higher shock strengths should shift the vulnerable period for T-wave shocks to shorter coupling intervals [4]. This hypothesis also has not yet been confirmed systematically.

* Corresponding author. Veterans Administrations Medical Center, 50 Irving St, NW, Washington, DC 20422, USA. Tel.: (+1-202) 745-8398; fax: (+1-202) 745-8184.

Time for primary review 48 days

PII S0008-6363(96)00058-2

d-Sotalol is an agent whose efficacy against ventricular arrhythmias is attributed to its action-potential-prolonging effect [10–15]. Whether *d*-sotalol alters the relation between repolarisation and the vulnerable period has not yet been tested.

The aims of the present study were (1) to determine the vulnerable period for electrical field shocks at 2 different shock strengths, one slightly above the fibrillation threshold and one close to the ULV, (2) to relate the coupling intervals and the durations of the vulnerable periods to the dispersion of 7 simultaneously recorded monophasic action potentials (MAPs) and to the T-wave of a volume-conducted ECG, and (3) to investigate the effects of *d*-sotalol on the dispersion of ventricular repolarisation and the associated vulnerable periods.

2. Methods

2.1. Preparation of isolated rabbit hearts

Nine hearts from white male New Zealand rabbits weighing 3.75 ± 0.48 kg were studied in accordance with the institution's review board. The investigation conformed with the *Guide for the Care and Use of Laboratory Animals* published by the US National Institute of Health (NIH publication No. 85-23, revised 1985). The animals were anesthetised with pentobarbital until their hind-reflexes to pain were depressed. The chest was opened and the heart was cut out. A cuff of intact aorta was left attached to the left ventricular outflow tract. The heart was immediately placed in iced Tyrode's solution. After removing the remaining pericardium and connective tissue, the aorta was cannulated and retrogradely perfused with Tyrode's solution. In addition to the normal ionic contents of Tyrode's solution, bovine albumin (0.6 mmol/l) and adenosine (0.1 μmol/l) were added to the perfusate [16]. The perfusion rate was adjusted to 35–45 ml/min, maintaining a perfusion pressure between 50 and 70 mmHg. The perfusate was equilibrated with 95% O_2 and 5% CO_2, the pH was adjusted to 7.4 ± 0.05 and the temperature of the perfusate was maintained at 37 ± 1°C. The high coronary flow rate and the special solution helped maintain a high physiological integrity and allowed us to obtain stable MAP signals and to extend the experimental protocol for up to 5 h. The time from excision of the heart to initiation of perfusion was less than 2 min. To slow the intrinsic heart rate, the AV node was ablated by mechanical pressure applied using a pair of surgical tweezers. The heart was mounted by suturing the right atrium on a modified vertical Langendorff apparatus. Fig. 1 shows a scheme of the experimental setup.

2.2. MAP recordings

Seven monophasic action potentials (MAPs) were recorded simultaneously using Franz Ag/AgCl contact

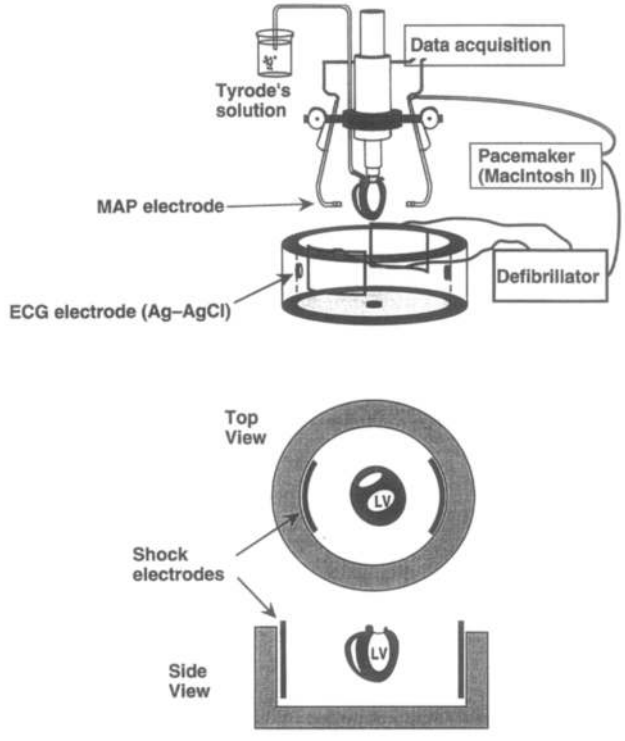

Fig. 1. Schematic picture of experimental setup, showing the heart mounted on a modified vertical Langendorff apparatus prior to immersion in the tissue bath. Two of 7 MAP catheters are shown mounted on the spring-loaded mechanism used for the epicardial MAP recordings. Shock electrode plates and ECG electrodes are located in the tissue bath. The computer delivered pacing stimuli through one of the endocardial MAP catheters and triggered the defibrillator at a programmed coupling interval after the last regularly paced beat. Data acquisition was performed simultaneously by the computer and a Gould strip chart recorder. The insets show the heart immersed in the tissue bath from top and side views. The left ventricular cavity is marked LV, and the positions of the shock electrodes are indicated.

MAP-pacing combination electrodes (EP Technologies, Sunnyvale, CA) capable of recording and pacing from the same catheter site [17,18]. MAPs were recorded simultaneously from 5 epicardial sites and 2 left ventricular endocardial sites. The epicardial recordings were located as follows: one on the right ventricular free wall, one on the right ventricle close to the posterior septum, two on the basal and apical left ventricular free wall and one on the left ventricle close to the anterior septum. The epicardial MAP electrodes were mounted on a custom-designed spring-loaded mechanism providing stable contact pressure [16]. The endocardial MAP recordings were obtained from standard 7-French MAP catheters (EP Technologies). Two endocardial MAP catheters were positioned at different sites on the left ventricular endocardium. Usually, MAP amplitudes were > 5 mV, with a minimal amplitude of 3.5 mV. Pacing was performed through one of the endocardial MAP catheters using a custom pacing program (LabVIEW II, version 2.2, National Instruments Inc., Austin, TX) run on a Macintosh IIfx computer, and a Bloom stimulus isolator (Bloom Inc., PA).

2.3. Recording of a volume-conducted ECG

ECG recordings were derived from 3 Ag/AgCl electrodes which were positioned at the walls and the bottom of the tissue bath in an approximate Einthoven configuration and referenced to a ground electrode in the tissue bath (Fig. 1). A standard ECG amplifier was used for signal amplification [16]. Of the 3 available 'limb leads', the lead with the longest monophasic T-wave was recorded [2]. An example of a simultaneous recording of 7 MAPs and the tissue bath ECG during steady-state pacing is shown in Fig. 2.

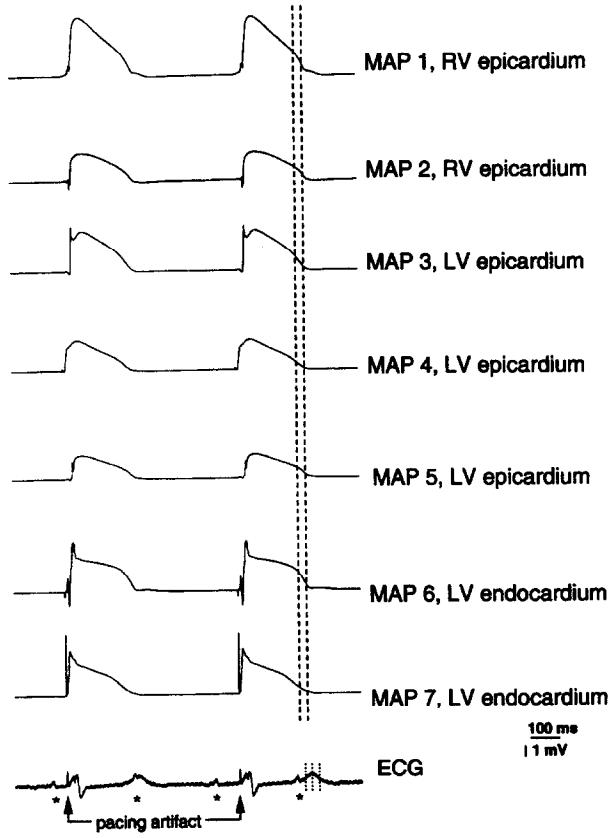

Fig. 2. Simultaneous recording of 7 monophasic action potentials (MAPs) and lead II of the tissue bath (volume-conducted) ECG during steady-state pacing at 600 ms cycle length. The upper 2 MAPs were recorded from the right ventricular epicardium, the middle 3 MAPs from the left ventricular epicardium, and the lower 2 from the left ventricular endocardium. The vertical lines to the left of each recording provide a 1 mV reference calibration for each MAP recording. The dotted lines mark the shortest repolarisation time (in MAP 7) and the longest repolarisation time (in MAP 1) at the 90% repolarisation level. The dispersion of repolarisation of the MAP recordings at 90% repolarisation is the interval between these lines. Arrows mark artifacts generated by pacing stimuli. Asterisks (*) mark P-waves in the ECG. The 3 dotted lines in the ECG recording mark the mid-upslope, peak and mid-downslope of the T-wave. Neither the mid-upslope nor the peak nor the mid-downslope of the T-wave coincided with the dispersion of 90% repolarisation as measured directly by the 7 MAPs.

2.4. Field shock application

Fibrillation and defibrillation shocks were delivered from an experimental defibrillator (Medtronics Model 2376) by means of two 5 × 5 cm rectangular stainless steel plate electrodes placed on opposite walls of the tissue bath (Fig. 1, inset). A clinically commonly used monophasic-waveform shock truncated at 5 ms was applied. The plate electrodes' size exceeded the dimensions of the centrally located heart in every direction, thus exposing the whole heart to the shock field. Measurements of the potential gradients in the tissue bath demonstrated a highly uniform shock field in the center of the bath where the heart was positioned. Since the impedance of the tissue bath and shock electrodes was low (between 10 and 12 Ω), a 10 Ω resistor was placed serially into the shock circuit. The waveform of the shock voltage was recorded on a digital oscilloscope (LeCroy, Model LS140) which automatically displayed peak and mean values and also recorded them to disk for off-line inspection. Delivered peak shock voltage was used as a measure of shock strength.

2.5. Protocol

The heart was paced at 600 ms basic cycle length from one of the two endocardial MAP catheters. This cycle length was both relatively long and guaranteed stable paced rhythms in all hearts without ectopic ventricular activity. The ULV and fibrillation threshold were estimated at the peak of the T-wave using an up-down protocol [19] in 50 V steps. Two voltages were scanned for the vulnerable period, one of them 50 V below the estimated ULV (high shock voltage), the other 50 V above the estimated fibrillation threshold (low shock voltage). Prior to delivery of the next shock, the heart was allowed to recover for 3 min if the shock did not induce VF, and for 5 min if the shock induced VF. Steady-state MAP durations were assessed prior to each shock. Experiments showing changes of steady-state MAP duration of more than 3% or MAP amplitude of more than 15% in more than 2 MAP recordings were excluded from the analysis.

2.6. Determination of the vulnerable period

To determine the vulnerable period for each of the two shock strengths, shocks were applied at different coupling intervals in steps of 5 ms. Coupling intervals were defined as the interval from the pacing artifact to the shock artifact and were verified by off-line analysis. The vulnerable period was scanned to determine the shortest and longest VF-inducing coupling interval. The contingency of the vulnerable period was tested by delivering shocks in coupling interval steps of $\leq$ 10 ms throughout the vulnerable period. The borders of the vulnerable period were determined with 5 ms accuracy. The duration of the vulnerable

period was calculated as the difference between the longest and the shortest coupling interval at which VF was induced. This procedure was repeated for the second shock strength. The order of determination of the 2 vulnerable periods was changed randomly.

Baseline data were verified by random reproduction of 6 previously delivered shocks. After completion of the baseline protocol, *d*-sotalol (Bristol-Myers Squibb, Inc.) was added to the perfusate at a concentration of 2×10^{-5} mol/l while the heart was continually paced at 600 ms cycle length. MAP durations were analyzed every 5 min. The protocol was repeated when ≥ 45 min drug loading time had elapsed and MAP prolongation by *d*-sotalol had reached a constant value at pacing with 600 ms cycle length for at least 5 min.

2.7. Data analysis

To allow for computer-aided analysis, MAP and ECG recordings were acquired digitally at a sampling rate of 1000 Hz by a custom computer program (LabVIEW II, version 2.2) run on a Macintosh II fx computer (Apple Computer Inc, Cupertino, CA). In addition, MAP and ECG recordings were acquired on a 8-channel strip chart recorder (Gould Model TA 4000, Gould Inc.) at a paper speed of 100 mm/s for manual analysis.

2.7.1. Direct analysis of dispersion of ventricular repolarisation by multiple MAP recordings

Using a validated computer algorithm (Franz et al., PACE, in press), MAPs were analyzed for action potential duration at 90, 70, and 50% repolarisation as the interval from the fastest MAP upstroke to the respective repolarisation level. The repolarisation level was determined relative to the plateau of the MAP. The plateau was defined as the part of the MAP showing the smallest first derivative (dV/dt) after the upstroke. The amplitude between the plateau and the diastolic potential was defined as 100% repolarisation. Action potential duration was analyzed from the fastest upstroke to 50, 70, and 90% repolarisation. Activation time was measured as the time between the pacing artifact and the fastest upstroke of the MAP. Repolarisation time was defined as the sum of activation time and action potential duration. Analysis was performed at least once every hour of the protocol during steady state. The dispersion of repolarisation was calculated by subtracting the minimal repolarisation time from the maximal repolarisation time recorded from the 7 MAP electrodes. The computer analysis was randomly verified by manual measurements of action potential durations at 50, 70, and 90% repolarisation and of activation time. Repolarisation was analyzed at 50, 70, and 90% as previous studies suggested that the late repolarisation phase might provide an arrhythmogenic substrate if exposed to electrical field shocks [20–22]. Analysis of MAP durations was performed in 20% steps as the difference between MAP durations at different repolarisation levels was then clearly bigger than the smallest difference in vulnerable period coupling intervals.

2.7.2. ECG wave analysis

Five ECG parameters were analyzed: (1) the QRS duration, (2) the time from the stimulus-evoked Q-wave (= pacing artifact in Fig. 2) to the mid-upslope of the T-wave, (3) the time from the Q-wave to the peak of the T-wave, (4) the time from the Q-wave to the mid-downslope of the T-wave, and (5) the time from the mid-upslope to the mid-downslope of the T-wave. The mid-upslope was defined as the time point when the ascending T-wave reached 50% of its maximal amplitude. The mid-downslope was defined as the time point when the descending T-wave returned to 50% of its maximal amplitude. The periods from the mid-upslope to the peak and from the mid-upslope to the mid-downslope of the T-wave were calculated.

2.8. Arrhythmia definitions

Due to its small myocardial mass, the rabbit heart is prone to recover spontaneously from an episode of induced VF. Previous observations in our laboratory [23] and that of others [24,25] revealed that more than 5 extra beats were consistently induced by shocks of coupling intervals and shock energies that induced sustained VF at least once. In addition, the ECG characteristics of the spontaneously terminating episodes lasting more than 5 extra beats were similar to the ECG of the episodes requiring external defibrillation. Therefore, VF and non-fibrillating episodes

Table 1
Shortest and longest coupling intervals (CI) of shocks inducing VF in 7 hearts

	Baseline shortest CI	Baseline longest CI	Baseline duration	*d*-Sotalol shortest CI	*d*-Sotalol longest CI	*d*-Sotalol duration
High shock strength	185 ± 13.9	226 ± 27.8	34.2 ± 11.6	214 ± 8.4	250 ± 17	36 ± 12.4
Low shock strength	201 ± 25.6	232 ± 24.7	30 ± 13.5	230 ± 17.6	265 ± 26.5	35 ± 16.5

The duration of the vulnerable period is calculated as the difference between the shortest and the longest coupling interval inducing VF. Data are presented for baseline conditions and after addition of *d*-sotalol, both for low and high shock strengths. Paired *t*-tests showed neither significant differences between the duration of the vulnerable periods for different shock strengths nor between baseline and *d*-sotalol data. All durations are given in ms as mean ± standard deviation. CI = coupling interval.

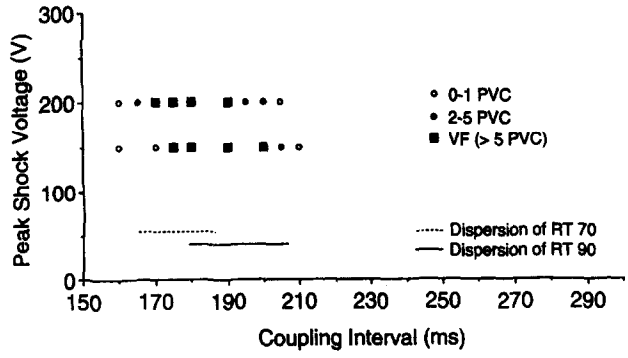

Fig. 3. Example for the 2 vulnerable periods determined in one heart at baseline. Each dot represents a delivered shock and indicates the shock coupling interval (x-axis), shock strength (y-axis) and the type of arrhythmia induced (coded by the dot type). Shocks that induced VF are indicated by large square solid symbols, shocks that induced non-sustained arrhythmias by small solid dots, and shocks that induced no arrhythmia by open dots. The bars at the bottom of the graph indicate the dispersion of repolarisation at 70% (RT 70, top bar, dashed line) and 90% (RT 90, bottom bar, solid line). The vulnerable periods coincide with the dispersion of repolarisation at 70% (vulnerable period for high shock strength) and 90% (vulnerable period for low shock strength).

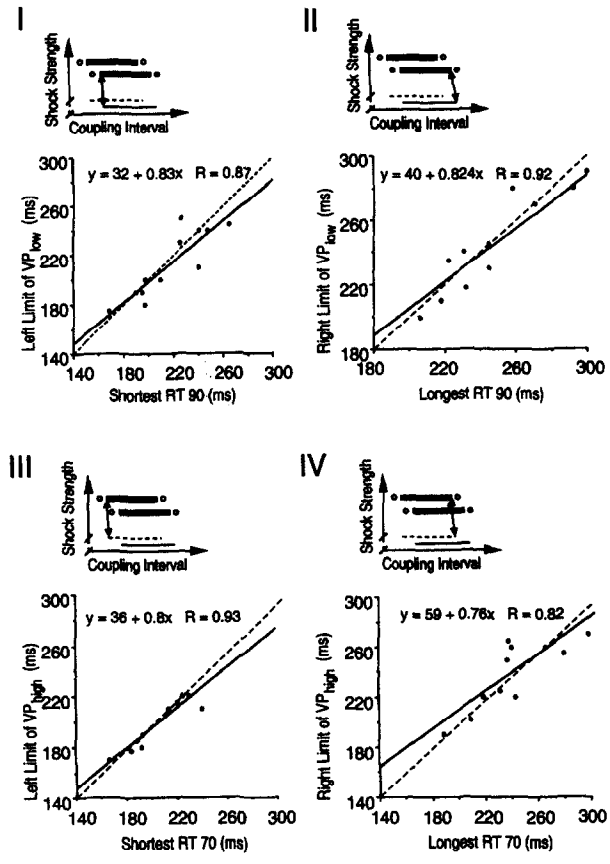

Fig. 4. Linear regressions of the left and right limits of the two vulnerable periods with the shortest and longest repolarisation times at 70 and 90% repolarisation for the combined baseline and d-sotalol data in 7 hearts. The correlations were highly significant ($P < 0.001$). Analysis of variance of the correlation coefficients showed that the regression lines were not significantly different from the line of identity ($P > 0.2$). The arrows in the insets visualize which measurements were correlated. *I*: Correlation of the left limit of the vulnerable period for low shock strengths (VP_{low}) with the shortest repolarisation time at 90% repolarisation (RT 90). *II*: Correlation of the right limit of the vulnerable period for low shock strengths with the longest repolarisation time at 90% repolarisation. *III*: Correlation of the left limit of the vulnerable period for high shock strengths (VP_{high}) with the shortest repolarisation time at 70% repolarisation (RT 70). *IV*: Correlation of the right limit of the vulnerable period for high shock strengths with the longest repolarisation time at 70% repolarisation.

were defined as follows: An episode was regarded as VF if at least 6 full excitations showing cycle lengths of less than 160 ms were induced by a shock in every MAP recording. Induction of 2 to 5 action potentials was regarded as non-sustained arrhythmia, and induction of 0 to 1 action potentials as no arrhythmia.

2.9. Statistical analysis

The dispersion of repolarisation at baseline and after addition of d-sotalol was compared using Student's paired t-test. The coupling intervals of the two vulnerable periods were also compared using the paired t-test. In order to relate the dispersion of repolarisation to the vulnerable periods, the shortest and longest repolarisation times at 50, 70, and 90% and the T-wave parameters were compared

Table 2
Shortest and longest activation times (AT), repolarisation times at 50% (RT 50), 70% (RT 70), and 90% (RT 90) repolarisation, and dispersion of repolarisation during steady-state pacing (600 ms cycle length) at baseline (left) and after addition of d-sotalol (right) in 7 hearts

	Baseline shortest	Baseline longest	Baseline dispersion	d-Sotalol shortest	d-Sotalol longest	d-Sotalol dispersion
AT	11.3 ± 6.6	40.8 ± 6.2	—	13.3 ± 13.5	43.9 ± 4.1	—
RT 50	166 ± 6.4	203 ± 15.1	38 ± 14.8	193 ± 17	235 ± 21.4	42 ± 18.7
RT 70	188 ± 13.4	220 ± 19	32.1 ± 11.4	218 ± 13.9	255 ± 21	36.7 ± 6.8
RT 90	201 ± 19.1	232 ± 16.8	31 ± 11.8	240 ± 17.6	277 ± 21	36.7 ± 16

The dispersion of repolarisation was calculated as the difference between the shortest and longest repolarisation time recorded in the 7 MAPs. Paired t-tests showed neither significant differences in dispersion between 50, 70, and 90% repolarisation, nor between repolarisation times at baseline and d-sotalol, nor in activation time between baseline and d-sotalol. All durations are given in ms as mean ± s.d.

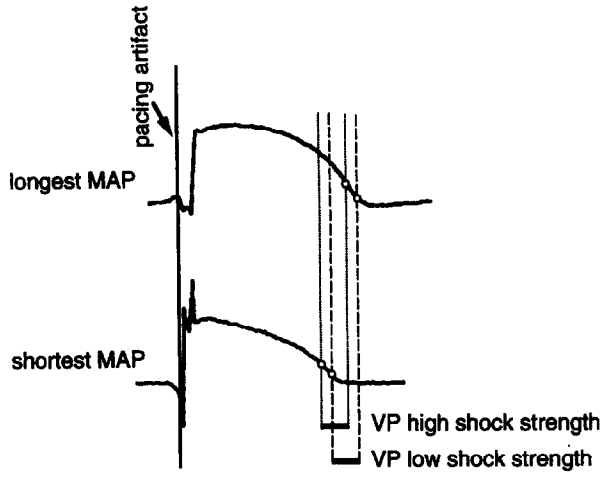

Fig. 5. Summary of the correlations between repolarisation and the vulnerable periods. Representative for the 7 MAP recordings, the MAPs showing the longest (top recording) and shortest (bottom recording) durations are plotted. The dashed lines mark the repolarisation times at 90%, and the dotted lines the repolarisation times at 70% repolarisation. The dispersion is therefore delineated by the interval between the two dotted lines for 70% repolarisation and between the two dashed lines at 90% repolarisation. Below, the vulnerable periods are marked by two horizontal lines for the high shock strength (VP high shock strength) and low shock strength (VP low shock strength). The vulnerable periods are determined by the dispersion of repolarisation at the corresponding repolarisation level.

with the left and right boundaries of the vulnerable periods using both paired *t*-tests and linear regression. These correlations enabled a comparison of the dispersion of repolarisation and the vulnerable periods in terms of duration and coupling interval referenced to the pacing stimulus. A *P*-value of < 0.05 was considered significant. All statistical tests were performed using the JMP software package for Macintosh (Version 2.05, SAS Institute Inc.).

3. Results

Sustained ventricular fibrillation (VF) was induced in 7 hearts and non-sustained VF lasting up to 17 beats in one. Shocks that induced VF were clustered within a discrete time interval for each of the 2 shock strengths. These intervals are referred to as the 'vulnerable periods'. Only shocks delivered within these vulnerable periods induced VF, and shocks delivered outside of the vulnerable periods did not induce VF. Each vulnerable period was bordered by a narrow transition zone (5–10 ms duration) during which shocks reproducibly induced 2–5 extra beats (2.7 ± 0.8 PVC, mean $\pm$ SD, Fig. 3). Shock strengths of the two vulnerable periods were 234 ± 90 V for the low and 294 ± 100 V for the high shock strength (mean $\pm$ s.d.).

3.1. Vulnerable period for low and high shock strengths

An example of vulnerable periods determined in one heart is shown in Fig. 3. The vulnerable period had a duration of 30 ± 14 ms for the low shock strength (range from 15 to 60 ms), and a duration of 34 ± 12 ms for the high shock strength (range from 20 to 50 ms, Table 1). There was no significant difference in the durations of the two vulnerable periods ($P > 0.2$). The shortest coupling interval inducing VF (left limit of the vulnerable period) was 16 ± 17 ms shorter for the high shock strength than for the low shock strength, and the longest coupling interval inducing VF (right limit of the vulnerable period) was 8 ± 12 ms shorter for the high shock strength than for the low shock strength ($P < 0.005$, Table 1). The vulnerable period was thus shifted leftward to shorter coupling intervals by the higher shock strength.

3.2. Dispersion of repolarisation

The dispersion of ventricular repolarisation was 31 ± 12 ms at 90% repolarisation (range from 20 to 47 ms), 32 ± 11 ms at 70% repolarisation (range from 21 to 60 ms), and 38 ± 15 ms at 50% repolarisation (range from 22 to 65 ms, P = NS, Table 2). Repolarisation times ranged from 201 ± 19 to 232 ± 17 ms at 90% repolarisation, from 188 ± 13 ms 220 ± 19 ms at 70% repolarisation, and from 166 ± 6 to 203 ± 15 ms at 50% repolarisation. All differences between repolarisation times at different repolarisation levels were significant ($P < 0.01$, Table 2).

3.3. Effects of d-sotalol

d-Sotalol shifted both vulnerable periods to longer coupling intervals by an average of 29 ± 15 ms ($P < 0.05$) for both the high and the low shock strength. The duration of the vulnerable periods remained unchanged (P = NS, Table 1). The shift of the vulnerable period to shorter coupling intervals by the high shock strength as compared to the low shock strength was still significant after infusion of *d*-sotalol (Table 1).

d-Sotalol prolonged the repolarisation time of all MAPs at 50, 70, and 90% repolarisation by 37, 37, and 40 ms, respectively (Table 2). The activation time remained unchanged after addition of *d*-sotalol. The dispersion of

Table 3
ECG intervals at baseline and after addition of *d*-sotalol at 600 ms cycle length in 7 hearts

	Baseline	*d*-Sotalol
QRS duration	18 ± 30	19 ± 32
Pacing spike to mid-upslope of T-wave	174.5 ± 22.5	244 ± 19.8
Pacing spike to peak of T-wave	220.1 ± 27.2	280.7 ± 17.5
Pacing spike to mid-downslope of T-wave	241 ± 28	302 ± 14.2
Mid-upslope to peak of T-wave	45.6 ± 8.3	36.2 ± 10.6
Mid-upslope to mid-downslope of T-wave	76.4 ± 9.8	57.5 ± 11.5

The mid-upslope of the T-wave was defined as the point when the T-wave reached 50% of its maximal amplitude, the peak of the T-wave as the point of maximal amplitude, and the mid-downslope of the T-wave as the point when the T-wave decreased to 50% of its maximal amplitude. All durations are given in ms as mean $\pm$ s.d.

repolarisation of the MAPs was not significantly changed by *d*-sotalol at any of the 3 repolarisation levels analyzed (Table 2) at the basic cycle length of 600 ms.

3.4. Correlation of vulnerable periods with dispersion of repolarisation

The left limit of the vulnerable period for the low shock strength coincided with the shortest repolarisation time at 90% repolarisation, and the left limit of the vulnerable period for the high shock strength coincided with the shortest repolarisation time at 70% repolarisation. Similarly, the right limit of the vulnerable period for the high shock strength coincided with the longest repolarisation time at 70% repolarisation, and the right limit of the vulnerable period for the low shock strength coincided with the longest repolarisation time at 90% repolarisation. The average differences were smaller than 10 ms and not significantly different from zero. In contrast, the shortest and longest repolarisation times at 50% repolarisation were shorter than the coupling intervals of either vulnerable period. The differences to the vulnerable period for high shock strengths amounted to 18 ± 9 ms between the shortest repolarisation time at 50% and its left limit, and to 20 ± 25 ms between the longest repolarisation time at 50% and its right limit (Tables 1 and 2). Linear regression analysis between the limits of the two vulnerable periods and the shortest and longest repolarisation times at 70 and 90% repolarisation using both baseline and *d*-sotalol data confirmed that (1) the shortest and longest repolarisation times at 90% repolarisation coincided with the vulnerable period for low shock strengths, and (2) that the shortest and longest repolarisation times at 70% repolarisation coincided with the vulnerable period for high shock strengths (Fig. 4). Fig. 5 summarizes these results graphically.

3.5. ECG data

The ECG data are summarized in Table 3. *d*-Sotalol prolonged repolarisation, as indicated by the prolonged intervals from the pacing artifact to the points on the T-wave measured. QRS duration and morphology was not changed by *d*-sotalol, indicating an essentially unchanged conduction velocity and activation sequence. Both vulnerable periods comprised the peak of the T-wave. The mid-upslope of the T-wave occurred within the vulnerable period for high shock strengths. The vulnerable period for the high shock strength began earlier than the mid-upslope of the T-wave and ended shortly after the peak of the T-wave. The vulnerable period for the low shock strength began before the peak of the T-wave and extended to coupling intervals shortly before the mid-downslope of the T-wave. The correlation between the right and left limits of the vulnerable periods and the T-wave parameters was weak ($r = 0.6$–0.72, intercept > 50 ms). The T-wave also did not provide a marker for the differentiation between the two vulnerable periods.

4. Discussion

The present investigation of the vulnerability of the myocardium to single shocks yielded several relevant findings: (1) The dispersion of ventricular repolarisation, as determined by multiple simultaneous MAP recordings, correlates closely with the vulnerable period to single electrical shocks. (2) Higher shock strengths shift the vulnerable period to the left (i.e., to shorter coupling intervals as measured from the pacing artifact to the shocks which induced VF). (3) The vulnerable period for low shock strengths just above the fibrillation threshold is approximated by the shortest and longest repolarisation time at the 90% level, while the vulnerable period for high shock strengths just below the ULV is approximated by the shortest and longest repolarisation time at the 70% level. The direct assessment of dispersion of ventricular repolarisation by multiple MAP recordings was found to be a better predictor of the vulnerable period than the T-wave of the surface ECG. (4) *d*-Sotalol prolonged MAP durations at multiple sites and shifted the vulnerable period to longer coupling intervals, without changing the dispersion of repolarisation or its correlation to the vulnerable periods.

4.1. Correlation of the vulnerable period with dispersion of repolarisation

A number of studies have reported an indirect link between the dispersion of repolarisation and the susceptibility to arrhythmias [1,26,27]. A correlation of the vulnerable period with the dispersion of repolarisation has previously been hypothesized for the induction of VF by a local stimulus [6,7,28]. The present study is the first to demonstrate a direct correlation between the vulnerable period for high energy field shocks and the dispersion of ventricular repolarisation measured by multiple MAP recordings.

Linear regression analysis and its resulting correlation coefficients can be more powerful if the independent variable (here, the dispersion of repolarisation) is modified in some ways. In this study we opted not to artificially modify dispersion of repolarisation (e.g., by regional ischemia) because this would have undermined the electrophysiological stability of the preparation. There was sufficient baseline dispersion of repolarisation within hearts and between hearts (20–60 ms) to allow for a statistically significant correlation of the limits of the vulnerable periods with the dispersion of repolarisation at the respective repolarisation levels.

4.2. Leftward shift of the vulnerable period with higher shock strengths

Previous studies referred to the vulnerable period to single electrical shocks without regard to possible changes of the vulnerable period by different shock strengths

[1,2,4,29]. The present study determined the vulnerable period for two different shock strengths, one close to the fibrillation threshold and one close to the ULV. The high shock strength caused a significant leftward shift of the vulnerable period to shorter coupling intervals, but did not affect its duration. Concordant with this leftward shift, the optimum correlation between the boundaries of the vulnerable period and the dispersion of repolarisation shifted from the 90% repolarisation level for low shock strengths to the 70% repolarisation level for high shock strengths. This is in keeping with the strength–interval relation [8,9,30], and with data showing that refractoriness, and partial and complete excitability of the myocardium, are closely related to its repolarisation level [31–33].

4.3. Mechanism of vulnerability to electrical field shocks

Epicardial mapping studies have related the induction of VF by a single shock to re-entry of multiple activation wave fronts in different patterns of multiple excitation and propagation [4,34–36]. A shock encountering tissue with dispersed repolarisation may induce new action potentials in regions with short repolarisation times and prolong action potentials in regions with long repolarisation times [21,37]. Thus, a globally applied field shock may initiate premature action potentials with slow conduction in some areas, while finding other areas refractory [21,37]. This is known to facilitate re-entry of multiple activation wave fronts and induction of VF [4,34]. The leftward shift of the vulnerable period with higher shock strengths can be explained accordingly. The myocardial responsiveness to higher shock strengths is increased in every region of the myocardium [8,9,30]. Due to this effect, a similar pattern of slow excitation and action potential prolongation may be induced by a shock applied at less complete repolarisation levels, and thus at shorter shock coupling intervals. Similarly, the vulnerable period would terminate earlier due to ubiquitous full excitation of the whole myocardium by the shock and subsequent termination of re-entrant activity due to conduction block. Shibata et al. reported that re-entry after induction of VF by T-wave shocks occurs in different regions for high strength shocks as compared to low shock strengths [4]. This finding is compatible with the present results, as the shortest MAP at 70% repolarisation was sometimes not the shortest MAP at 90% repolarisation, due to different repolarisation slopes. Further studies of the origin of re-entry arrhythmias induced by T-wave shocks, using bipolar epicardial mapping and MAP recordings simultaneously, may provide an even deeper understanding of the VF-inducing mechanism.

4.4. Correlation of the vulnerable period with T-wave parameters

The coupling intervals of shocks inducing VF for clinical determination of the defibrillation threshold and the upper limit of vulnerability are usually determined by analyzing the T-wave of the surface ECG [2,5,28]. Our study confirmed the approximate concurrence of the vulnerable period with the mid-upslope and the peak of the T-wave [2,28]. However, the T-wave was not as strong a predictor of the vulnerable period as was the dispersion of repolarisation measured by multiple MAP recordings. The T-wave also did not differentiate between the vulnerable period for high and low shock strengths. It has been reported recently that the vulnerable period concurs with the downslope of the T-wave in some animal models [5]. This group explained the different relation of the vulnerable period and the T-wave by different defibrillator lead configurations. In addition, this difference might have been due to the lesser accuracy of the T-wave in delineating the dispersion of repolarisation and the vulnerable period.

4.5. Effects of d-sotalol

In accordance with previous observations, *d*-sotalol prolonged the action potential duration [12,13,38]. Prolongation was seen at all MAP recording sites in this study. This was associated with a shift of both the dispersion of repolarisation and the vulnerable periods to longer coupling intervals. The range of dispersion of repolarisation and the spread of the vulnerable periods were not affected by *d*-sotalol, nor was the correlation between the two. The reduction of QT-dispersion by the racemate, *dl*-sotalol, in patients [10,39,40] can therefore not be explained by the present findings in the isolated heart, and may rather be attributed to modification of other factors influencing dispersion in the in situ heart (e.g., autonomic influences or response to heart rate changes). Experimental studies showed that *d*-sotalol does not alter vulnerability, whereas *dl*-sotalol increases the defibrillation threshold [15]. In accordance with those results, the present study did not show an alteration of arrhythmia vulnerability by *d*-sotalol. The premature ending of the SWORD trial [41] due to a lack of antiarrhythmic action of *d*-sotalol concurs with these results.

4.6. Methodological considerations

A limitation of the isolated rabbit heart model is its tendency to spontaneously convert from induced VF [24,42]. The definition of VF used in this study follows that of several other groups [24,43] and was confirmed by two observations in this study. (1) The highest number of extra beats induced in the non-sustained arrhythmia group was 3.7 ± 1 PVC (range from 1 to 5), while the lowest number of extra beats in the VF group was 10.2 ± 7 PVC (range from 6 to 30), showing a sharp increase (6.4 ± 7 PVC) in the number of extra beats induced above 5 PVC. (2) ECG characteristics were similar between episodes of non-sustained and sustained VF.

While the correlations of repolarisation times at 70%

with the vulnerable period for high shock strengths and at 90% with the vulnerable period for low shock strengths were excellent in this study (Fig. 4), repolarisation times at different repolarization levels will probably yield similar correlations with vulnerable periods for different shock strengths.

The ventricular rabbit heart cell has different channel distributions from the human heart [44], resulting in a different shape of the electrical restitution curve [45]. In addition, our preparation was deprived of autonomic influences. The results obtained in this study therefore require validation in the human heart prior to clinical application.

4.7. Practical implications

The close correlation between vulnerability and dispersion of repolarisation conversely implies that, in anesthetised animals, a series of T-wave shocks could be used to scan the vulnerable period and consequently to infer the dispersion of repolarisation. This would allow for non-invasive testing of the effects of antiarrhythmic drugs and autonomic changes on the dispersion of repolarisation. In an investigative setting which allows multiple VF inductions, this method can provide accurate, non-invasive estimates of the dispersion of ventricular repolarisation.

Acknowledgements

The authors wish to thank Drs. Günter Breithardt and Martin Borggrefe, Westfälische Wilhelms-Universität, Münster, Germany, and Dr. Ross Fletcher, VA Medical Center, Washington, DC, USA, for their continuing support for this work.

References

[1] Wiggers CJ, Wegren, R. Ventricular fibrillation due to single localized induction in condenser shock supplied during the vulnerable phase of ventricular systole. Am J Physiol 1940;128:500–505.
[2] Chen PS, Feld GK, Kriett JM, et al. Relation between upper limit of vulnerability and defibrillation threshold in humans. Circulation 1993;88:186–192.
[3] Chen PS, Wolf PD, Ideker RE. Mechanism of cardiac defibrillation. A different point of view. Circulation 1991;84:913–919.
[4] Shibata N, Chen PS, Dixon EG, et al. Influence of shock strength and timing on induction of ventricular arrhythmias in dogs. Am J Physiol 1988;255:H891–H901.
[5] Walker RG, Idriss SF, Malkin RA, Ideker RE. Comparison of methods for determining the upper limit of vulnerability. Circulation 1993;88:I-593(Abstract).
[6] Burgess MJ. Relation of ventricular repolarization to electrocardiographic T wave-form and arrhythmia vulnerability. Am J Physiol 1979;236:402.
[7] Zipes DP. Electrophysiological mechanisms involved in ventricular fibrillation. Circulation 1975;52:120–130.
[8] Michelson EL, Spear JF, Moore EN. Strength–interval relations in a chronic canine model of myocardial infarction. Implications for the interpretation of electrophysiologic studies. Circulation 1981;63:1158–1165.
[9] Davidenko JM, Levi RJ, Maid G, Elizari MV, Rosenbaum MB. Rate dependence and supernormality in excitability of guinea pig papillary muscle. Am J Physiol 1990;259:H290–H299.
[10] Hohnloser SH, Woosley RL. Sotalol. N Engl J Med 1994;331:31–38.
[11] Roden DM. Usefulness of sotalol for life-threatening ventricular arrhythmias. Am J Cardiol 1993;72:51A–55A.
[12] Brachmann J, Beyer T, Schmitt C, et al. Electrophysiologic and antiarrhythmic effects of *d*-sotalol. J Cardiovasc Pharmacol 1992;20:S91–S95.
[13] Huikuri HV, Yli-Mayry S. Frequency dependent effects of *d*-sotalol and amiodarone on the action potential duration of the human right ventricle. Pace Pacing Clin Electrophysiol 1992;15:2103–2107.
[14] Schwartz J, Crocker K, Wynn J, Somberg JC. The antiarrhythmic effects of *d*-sotalol. Am Heart J 1987;114:539–544.
[15] Kwan YW, Solca AM, Gwilt M, Kane KA, Wadsworth RM. Comparative antifibrillatory effects of *d*- and *dl*-sotalol in normal and ischaemic ventricular muscle of the cat. J Cardiovasc Pharmacol 1990;15:233–238.
[16] Franz MR, Cima R, Wang D, Profitt D, Kurz R. Electrophysiological effects of myocardial stretch and mechanical determinants of stretch-activated arrhythmias [published erratum appears in Circulation 1992 Nov;86(5):1663]. Circulation 1992;86:968–978.
[17] Franz MR, Burkhoff D, Spurgeon H, Weisfeldt ML, Lakatta EG. In vitro validation of a new cardiac catheter technique for recording monophasic action potentials. Eur Heart J 1986;7:34–41.
[18] Franz MR, Chin MC, Sharkey HR, Griffin JC, Scheinman MM. A new single catheter technique for simultaneous measurement of action potential duration and refractory period in vivo. J Am Coll Cardiol 1990;16:878–886.
[19] Cha YM, Peters BB, Birgersdotter-Green U, Chen PS. A reappraisal of ventricular fibrillation threshold testing. Am J Physiol 1993;264:H1005–H1010.
[20] Zhou XH, Knisley SB, Wolf PD, Rollins DL, Smith WM, Ideker RE. Prolongation of repolarization time by electric field stimulation with monophasic and biphasic shocks in open-chest dogs. Circ Res 1991;68:1761–1767.
[21] Knisley SB, Smith WM, Ideker RE. Effect of field stimulation on cellular repolarization in rabbit myocardium. Implications for reentry induction. Circ Res 1992;70:707–715.
[22] Dillon SM. Synchronized repolarization after defibrillation shocks. A possible component of the defibrillation process demonstrated by optical recordings in rabbit heart. Circulation 1992;85:1865–1878.
[23] Kirchhof PF, Fabritz CL, Zabel M, Franz MR. The field of cardiac vulnerability: a two-dimensional definition of inducibility of ventricular fibrillation. Circulation 1994;90:I-182(Abstract).
[24] MacConaill M. Ventricular fibrillation thresholds in Langendorff perfused rabbit hearts: all or none effect of low potassium concentration. Cardiovasc Res 1987;21:463–468.
[25] Jones DL, Klein GJ, Gulamhusein S, Jarvis E. The repetitive ventricular response: relationship to ventricular fibrillation threshold in dogs. Pace Pacing Clin Electrophysiol 1983;6:1258–1267.
[26] Brugada J, Brugada P, Boersma L, et al. On the mechanisms of ventricular tachycardia acceleration during programmed electrical stimulation. Circulation 1991;83:1621–1629.
[27] Taggart P, Sutton P, Lab M, Dean J, Harrison F. Interplay between adrenaline and interbeat interval on ventricular repolarisation in intact heart in vivo. Cardiovasc Res 1990;24:884–895.
[28] Lesigne C, Levy B, Saumont R, Birkul P, Bardou A, Rubin B. An energy–time analysis of ventricular fibrillation and defibrillation thresholds with internal electrodes. Med Biol Eng 1976;14:617–622.
[29] Kolman BS, Verrier RL, Lown B. The effect of vagus nerve stimulation upon vulnerability of the canine ventricle: role of sympathetic–parasympathetic interactions. Circulation 1975;52:578–585.
[30] Langberg JJ, Calkins H, Sousa J, El-Atassi R, Morady F. Effects of

drive train stimulus intensity on ventricular refractoriness in humans. Circulation 1991;84:181–187.

[31] Franz MR, Swerdlow CD, Liem LB, Schaefer J. Cycle length dependence of human action potential duration in vivo. Effects of single extrastimuli, sudden sustained rate acceleration and deceleration, and different steady-state frequencies. J Clin Invest 1988;82:972–979.

[32] Franz MR, Costard A. Frequency-dependent effects of quinidine on the relationship between action potential duration and refractoriness in the canine heart in situ. Circulation 1988;77:1177–1184.

[33] Fabritz CL, Kirchhof PF, Zabel M, Franz MR. Higher shock strengths decrease the dispersion of post-shock activation and recovery times: an explanation of the upper limit of vulnerability. Circulation 1994;90:I-412(Abstract).

[34] Chen PS, Wolf PD, Dixon EG, et al. Mechanism of ventricular vulnerability to single premature stimuli in open-chest dogs. Circ Res 1988;62:1191–1209.

[35] Frazier DW, Wolf PD, Wharton JM, Tang AS, Smith WM, Ideker RE. Stimulus-induced critical point. Mechanism for electrical initiation of reentry in normal canine myocardium. J Clin Invest 1989;83:1039–1052.

[36] Zhou X, Daubert JP, Wolf PD, Smith WM, Ideker RE. Epicardial mapping of ventricular defibrillation with monophasic and biphasic shocks in dogs. Circ Res 1993;72:145–160.

[37] Dillon SM. Optical recordings in the rabbit heart show that defibrillation strength shocks prolong the duration of depolarization and the refractory period. Circ Res 1991;69:842–856.

[38] Kidwell GA, Gonzalez MD. Effects of flecainide and *d*-sotalol on myocardial conduction and refractoriness: relation to antiarrhythmic and proarrhythmic drug effects. J Cardiovasc Pharmacol 1993;21:621–632.

[39] Day CP, McComb JM, Matthews J, Campbell RWF. Reduction in QT dispersion by sotalol following myocardial infarction. Eur Heart J 1991;12:423–427.

[40] Campbell RWF, Furniss SS. Practical considerations in the use of sotalol for ventricular tachycardia and ventricular fibrillation. Am J Cardiol 1993;72:80A–85A.

[41] Waldo AL, Camm AJ, deRuyter H, Friedman J, MacNeill DJ, Pitt B. Preliminary mortality results from the survival with oral *d*-sotalol (SWORD) trial. J Am Coll Cardiol 1995 1995;25:15A(Abstract).

[42] Merillat JC, Lakatta EG, Hano O, Guarnieri T. Role of calcium and the calcium channel in the initiation and maintenance of ventricular fibrillation. Circ Res 1990;67:1115–1123.

[43] Cooper RA, Alferness CA, Smith WM, Ideker RE. Internal cardioversion of atrial fibrillation in sheep. Circulation 1993;87:1673–1686.

[44] Brown HF, Noble D, Noble SJ, Taupignon AI. The relationship between the transient inward current (TI) and other components of slow inward current in mammalian cardiac muscle. Jpn Heart J 1986;1:127–142.

[45] Kurz RW, Ren XL, Franz MR. Dispersion and delay of electrical restitution in the globally ischaemic heart. Eur Heart J 1994;15:547–554.